CHAPTER IV
RESULTS AND DISCUSSION

4.1 Zeolite properties

Among the zeolite used in this work as referred to Table 3.1, LTA-type zeolites (NaA, AgA, and CaA) have the highest aluminum content (Si/Al = 1.0), followed by NaX (Si/Al = 1.3), NaY (Si/Al = 2.5) and beta (Si/Al = 16.0). Silicalite has the lowest aluminum content (Si/Al = 196). This suggests that hydrophilicity of these zeolites increase in the order of silicalite < beta < NaY < NaX < NaA ≈ AgA ≈ CaA.

In this work, NaX and NaY, were selected to study the influence of Si/Al ratio in CO_2/CH_4 separation. Since these two zeolites have the same zeolitic framework but with different aluminum contents. In addition, the effects of hydrophobic/hydrophilic nature of zeolite framework on CO_2/CH_4 separation performance were studied by incorporating silicalite and beta zeolite into CA. LTA-type zeolites were chosen to examine both the molecular sieving and facilitated transport effects. Moreover, the number of literature involving mordenite zeolite incorporated into polymer matrix is still limited. Hence, the gas separation performance of MOR-CA MMMs was also explored.

4.2 CO_2 permeance and CO_2/CH_4 separation performance of pure CA membranes

Due to the condensable nature of CO_2 and its good interaction with the polar segments of CA, pure CA membranes are more selective to CO_2 than CH_4 where its values of α_{CO_2/CH_4} are 11.30 and 11.50 at 50 and 100 psi, respectively. Both of which are much greater than unity. An increase in feed pressure results in a slightly increase in both CO_2 permeance and CO_2/CH_4 selectivity. This is because an increase in driving force for gas permeation through MMMs is more pronounced for fast gas component (CO_2) than slower one (CH_4).

4.3 Effect of Si/Al ratio on CO_2/CH_4 separation performance

NaY-CA and NaX-CA MMMs were successfully fabricated with different zeolite loadings (up to 40% zeolite loading). Their CO_2 permeances at 50 and 100 psi feed pressures are shown in Figure 4.1.

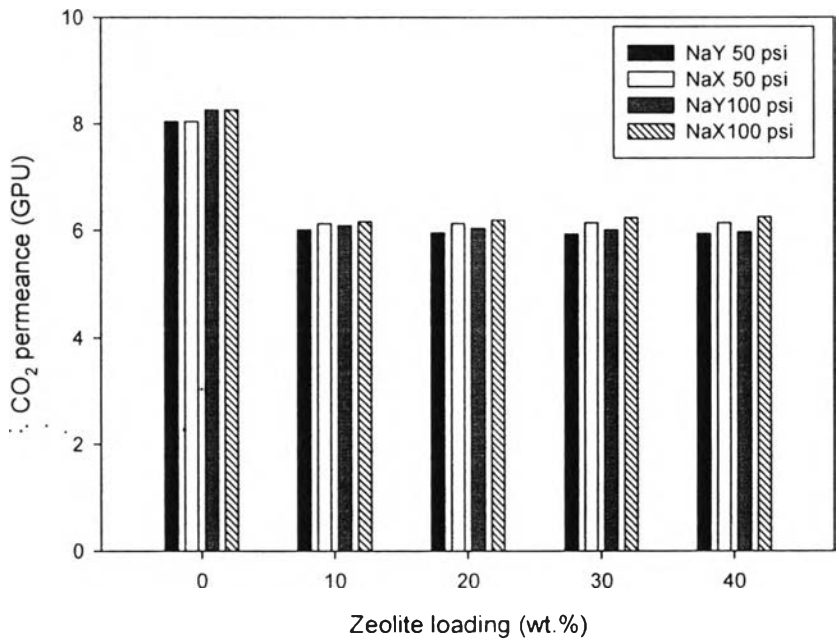

Figure 4.1 Effects of NaY and NaX loadings on CO_2 permeance at 50 and 100 psi feed.

The incorporation of NaY and NaX into CA polymer matrix results in a drop-off in CO_2 and CH_4 permeances as compared to those of pure CA membranes. This is because the presence of NaY and NaX disturbs the transient gap of polymer chains. This transient gap allows penetrant molecules to pass through polymer matrix. The existence of NaY and NaX obstructs the movement of the nearby CA chains and reduces CA chain mobility. Hence, CO_2 molecules are more difficult to penetrate through the membrane (Charoenpol, 2002).

As NaY and NaX loadings were increased from 10% to 40%, CO_2 permeance was not enhanced. This is because the pore opening of faujasite zeolite (7.4 Å) is larger than kinetic diameters of both CO_2 and CH_4 molecules. Thus, NaY and NaX did not play

any molecular sieving effect on CO_2 and CH_4, allowing both gases to freely pass through them. However, due to the preferential interaction between the electric field gradient of NaX and the permanent electric quadrupole moment of CO_2, the permeance of CO_2 of NaX-CA MMMs is somewhat higher than that of NaY-CA MMMs.

It is obviously shown in the Figure 4.1 that an increase in feed pressure from 50 to 100 psi could not improve the CO_2 permeance. This implies that the negative effect of polymer chain rigidification, caused by the presence of molecular sieve in the polymer matrix, can compensate the increase in driving force resulted from an increase in feed pressure across the membrane for gas molecules to penetrate through MMMs.

The CO_2/CH_4 selectivities for NaY and NaX at different loadings are shown in Figure 4.2. It shows that the incorporation of NaY into the membrane resulted did not enhance CO_2/CH_4 selectivity when compared to that of CA membrane. As discussed previously, this is due to its large pore opening compared to kinetic diameter of CO_2 and CH_4 molecules, NaY zeolite can not discriminate the difference between CO_2 and CH_4 molecules, or molecular sieving mechanism of NaY plays a minor role in CO_2/CH_4 separation. As a result, the magnitude of CO_2/CH_4 selectivity of NaY-CA MMMS is comparable to that of pure CA membranes.

In contrast, NaX-CA MMMs were improved for CO_2/CH_4 separation performance at a maximum NaX loading of 20%, as shown in Figure 4.2. This superior to CO_2/CH_4 separation performance of NaX-CA MMMs is attributed to the nature of NaX framework. Due to the lower Si/Al ratio compared to that of NaY zeolite, the framework of NaX zeolite possesses higher electric field gradients, generated by an asymmetrically distribution of the negatively charged framework and positively charged in the structure, which can strongly interact with the permanent electric quadrupole moment of CO_2 molecules and are able to selectively attract CO_2 molecules than CH_4 molecules as compared to those of NaY-CA MMMs. However, as NaX zeolite was further added into CA polymer matrix, the decrease in CO_2/CH_4 separation performance was attributed to the strong interactions between CO_2 and NaX zeolite resulting in obstructing other CO_2 molecules to pass freely through the MMMs.

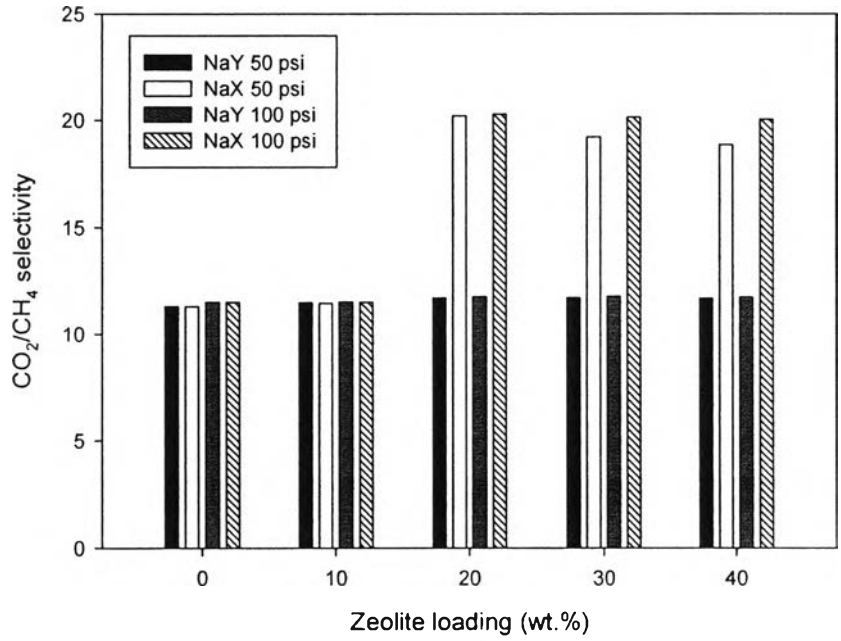

Figure 4.2 Effects of NaY and NaX loadings on CO_2/CH_4 selectivity at 50 and 100 psi feed.

The comparison of CO_2 permeances between silicalite and beta loadings at 50 and 100 psi feed pressures illustrated in Figure 4.3 shows that at a given zeolite loading, an increase in feed pressure from 50 to 100 psi did not enhance CO_2/CH_4 selectivity. This implies that the separation performance of NaY-CA and NaX-CA MMMs does not depend on the feed pressure in the studied range.

Additionally, the effect of Si/Al ratio on CO_2/CH_4 separation performance was studied by introducing the silicalite and beta zeolites into CA polymer matrix. As illustrated in Figures 4.3 and 4.4, neither CO_2 permeance nor CO_2/CH_4 selectivity of both MMMs was improved when increased zeolite loading. This is due to the synergetic effect between the hydrophobic framework and the asymmetrical pore opening of the zeolites in that the hydrophobic framework tends to repulse CO_2 molecules while the asymmetrical pore opening impedes CH_4 molecules to pass through them (Huang *et al.*, 2006). This means that transport property and membrane separation performance of both MMMs are not only influenced by hydrophobic property but also by the characteristic sinuous chan-

nel system. Nevertheless, it should be noted that at a given zeolite content, the CO_2 permeance of beta-CA MMMs is higher than that of silicalite-CA MMMs. This trend can be explained in terms of pore opening of both zeolites. Since the pore apertures of silicalite and beta are 5.2×5.7 $Å^2$ and 7.1×7.3 $Å^2$, the larger dimension of beta pore opening allows more CO_2 molecules to transport through beta-CA MMMs, resulting in the higher CO_2 permeance as compared to silicalite-CA MMMs.

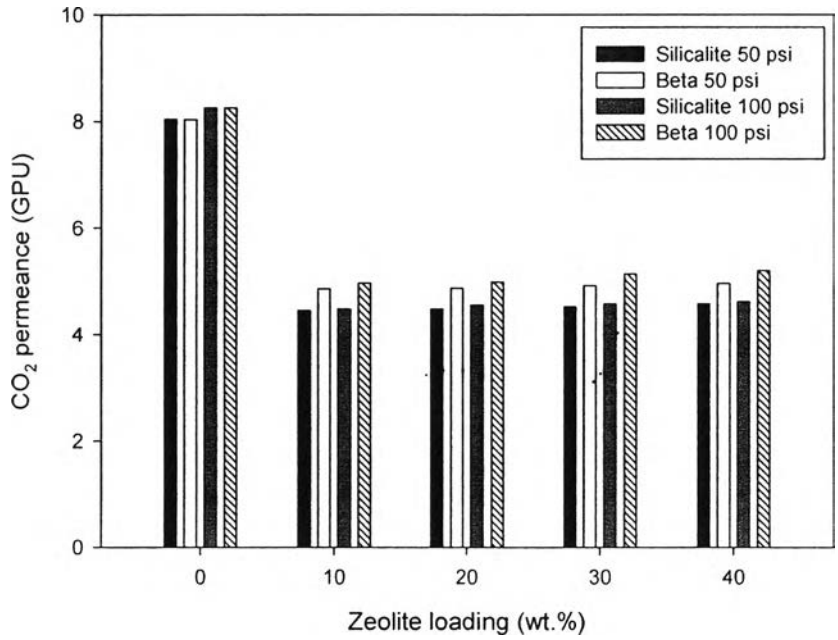

Figure 4.3 Effects of silicalite and beta loadings on CO_2 permeance at 50 and 100 psi feed.

As seen in Figure 4.4, the comparison of CO_2/CH_4 selectivities between silicalite and beta loadings at 50 and 100 psi reveals that CO_2/CH_4 separation performance of silicalite-CA MMMs and beta-CA MMMs is independent of the feed pressure. This means that an increase in molecular driving force for gas molecules to penetrate through MMMs does not affect the separation performance of both MMMs.

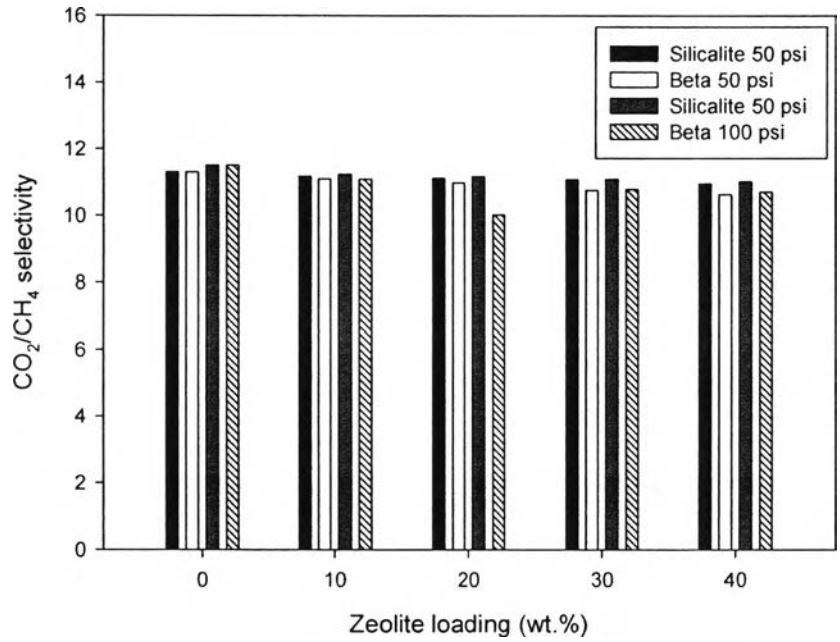

Figure 4.4 Effects of silicalite and beta loadings on CO_2/CH_4 selectivity at 50 and 100 psi feed.

4.4 Effect of cation on CO_2/CH_4 separation performance

LTA-typed zeolites, NaA and AgA, were chosen for investigating the effect of Ag^+ on CO_2/CH_4 separation performance. NaA-CA and AgA-CA MMMs were fabricated with different zeolite loadings (up to 40% zeolite loading).

CO_2 permeances of AgA-CA MMMs compared to that of NaA-CA MMMs are shown in Figure 4.5. The results show that CO_2 permeance of AgA-CA MMMs is much higher than that of NaA-CA MMMs at the feed pressure and a given zeolite loading. Moreover, CO_2 permeances of both MMMs were decreased with an increase in zeolite loading.

Theoretically, the pore size of AgA zeolite would be slightly smaller than that of NaA zeolite (3.8 Å) because the silver ionic radius (1.15 Å) is greater than that of sodium ionic (1.02 Å). Since the kinetic diameter of CH_4 molecules is approximately 3.8 Å; hence, the molecular sieving mechanism may play a role in decreasing CH_4 permeance of

AgA-CA MMMs (Li *et al.*, 2007). However, the kinetic diameter of CO_2 molecules (3.3 Å) is smaller than the pore sizes of both NaA and AgA. Furthermore, the double bond in CO_2 molecules can reversibly react with Ag^+ forming a π-bonded complex. Such a complex facilitates CO_2 to pass through AgA zeolite. The transition metals or their ions can form σ-bonds to carbons or form bonds with the unsaturated hydrocarbons in a non-classical manner called π-backbonding which is a unique characteristic of the transition metals. Thus, the facilitated transport mechanism is a main influence attributed to the higher CO_2 permeance of AgA-CA MMMs compared to that of NaA-CA MMMs.

A decrease in CO_2 permeance with increasing zeolite loading was attributed to the polymer chain rigidification induced by the presence of nearby molecular sieve (Mahajan, 2000, and Li *et al.*, 2005 and 2006). This implies that in the case of AgA-CA MMMs, the facilitated transport mechanism cannot compensate a negative effect of polymer chain rigidification.

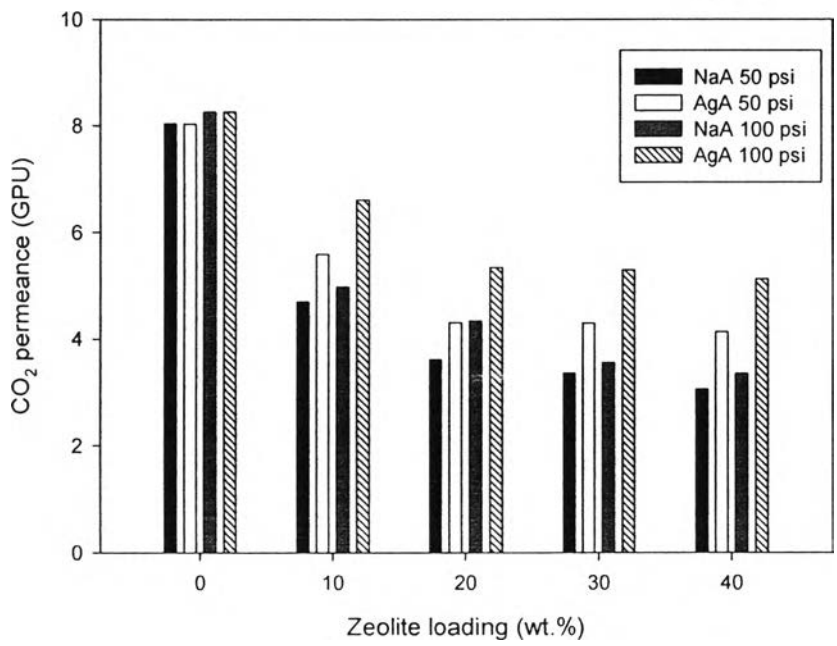

Figure 4.5 Effects of NaA and AgA loadings on CO_2 permeance at 50 and 100 psi feed.

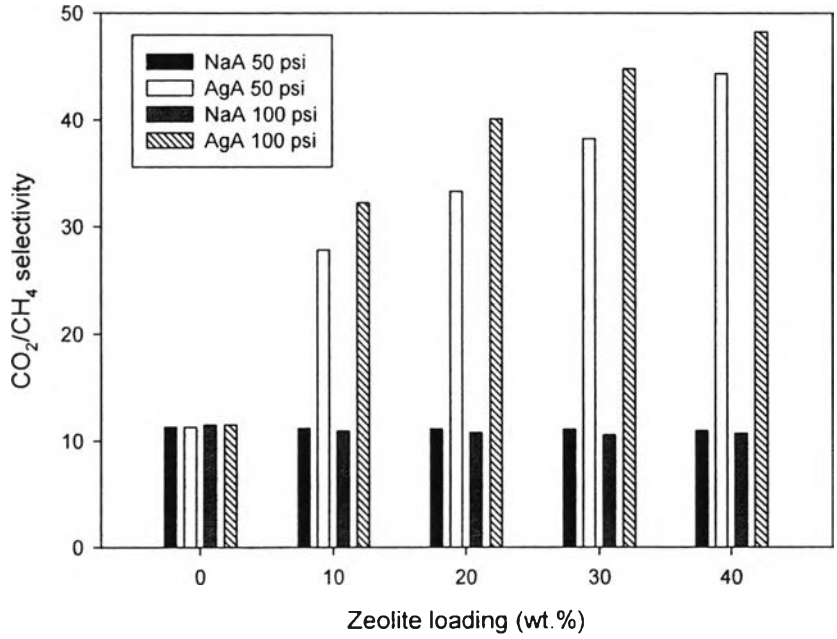

Figure 4.6 Effects of NaA and AgA loadings on CO_2/CH_4 selectivity at 50 and 100 psi feed.

The CO_2 permeances of NaA-CA MMMs and AgA-CA MMMs are enhanced with increasing in feed pressure. This means that an increase in molecular driving force for gas molecules to penetrate through MMMs can overcome the polymer chain rigidification effect.

Figure 4.6 illustrates that CO_2/CH_4 selectivity of AgA-CA MMMs increases with an increase in zeolite loading whereas that of NaA-CA MMMs does not improve. This is due to the synergetic effect of the facilitated transport mechanism of Ag^+ and the molecular sieving mechanism of zeolite as previously discussed. Moreover, as increased in feed pressure, the separation performance of AgA-CA MMMs is improved.

4.5 Effect of pore size on CO_2/CH_4 separation performance

NaA and CaA zeolites posses similar physical properties but differ in the pore opening.

NaA-CA and CaA-CA MMMs with different zeolite loadings were prepared by the solution-casting method. The effect of zeolite loading on the permeance of tested gases for NaA-CA and CaA-CA MMMs is shown in Figure 4.7. The results show that CO_2 permeance of CaA-CA MMMs is somewhat higher than that of NaA-CA MMMs at a given zeolite loading. Moreover, permeances of all studied gases are decreased with increasing zeolite loading. Although the magnitude of gas permeance and their variations with zeolite loadings are different for different tested gases, the general trend is similar to which it implies a similar permeation mechanism. Since, the pore sizes of NaA and CaA are larger than the kinetic diameters of CH_4 and CO_2, the decreasing trend of permeability seems to be so strange. However, a decrease in permeance may be attributed to a decrease in mobility of polymer chains near the polymer-zeolite interface as previously discussed.

Figure 4.7 also reveals that at a given zeolite loading, CO_2 permeance is increased with an increase in zeolite pore size (from NaA to CaA zeolite). This is because the larger the zeolite pore size, the easier the gas penetration is. Furthermore, the CO_2/CH_4 selectivity was raised with an increase in zeolite pore size as shown in Figure 4.8. Actually, these evidences strongly support the partial pore blockage of zeolites by polymer chains (Moored (2004) and Li *et al.*, (2005 and 2006)). This phenomenon plays an important role in gas separation performance of CA-zeolite MMMs. If a molecular sieving mechanism governs the separation efficiency, the CO_2/CH_4 selectivity of NaA-CA MMMs should be greater than that of CaA-CA MMMs. This demonstrates that the partial pore blockage of zeolites by the polymer chains has an influence on the separation performance of MMMs as well as the polymer chain rigidification.

In addition, an increase in feed pressure facilitates CO_2 molecules (fast gas) rather than CH_4 molecules.

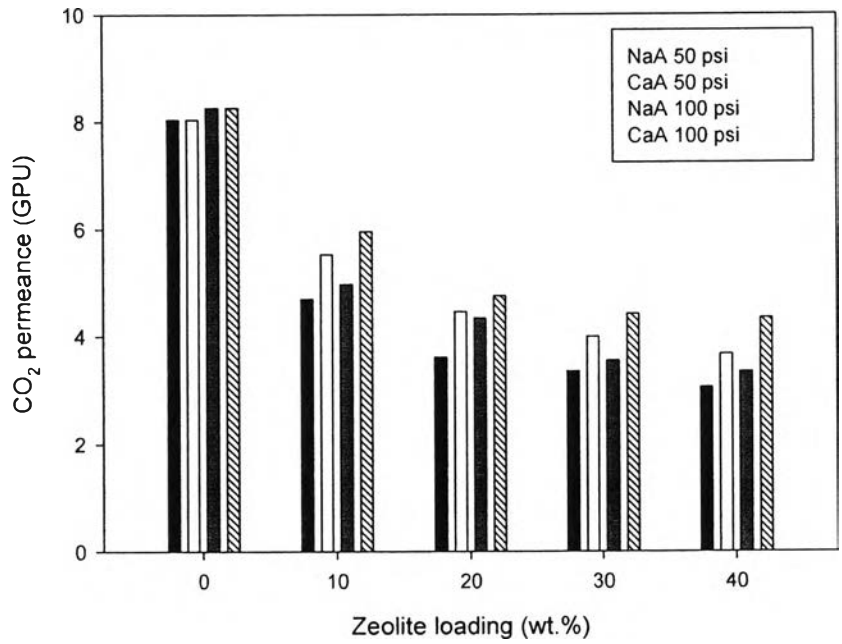

Figure 4.7 Effects of NaA and CaA loadings on CO_2 permeance at 50 and 100 psi feed.

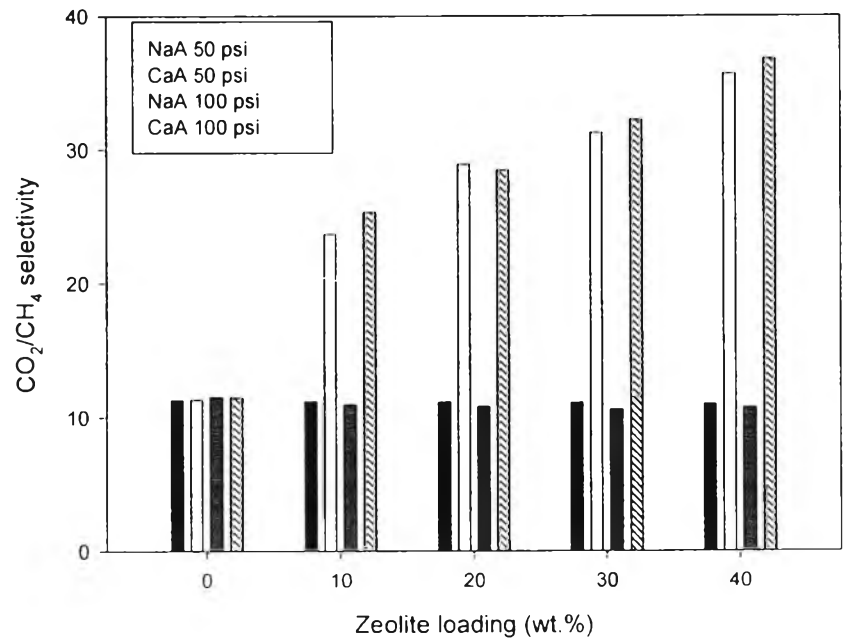

Figure 4.8 Effects of NaA and CaA loadings on CO_2/CH_4 selectivity at 50 and 100 psi feed.

4.6 Mordenite-CA MMMS

Since a number of research work related to the mordenite zeolite incorporated into a continuous polymer phase is still limited, it is promising to extensively examine the effect of adding mordenite to CA polymer matrix on CO_2/CH_4 separation performance.

Mordenite-CA MMMs (MOR-CA MMMs) were successfully fabricated with different zeolite loadings (up 40% zeolite loading). The CO_2 permeance of MOR-CA MMMS is shown in Figure 4.9. The CO_2/CH_4 separation performance of MOR-CA MMMs at different mordenite loadings is illustrated in Figure 4.10.

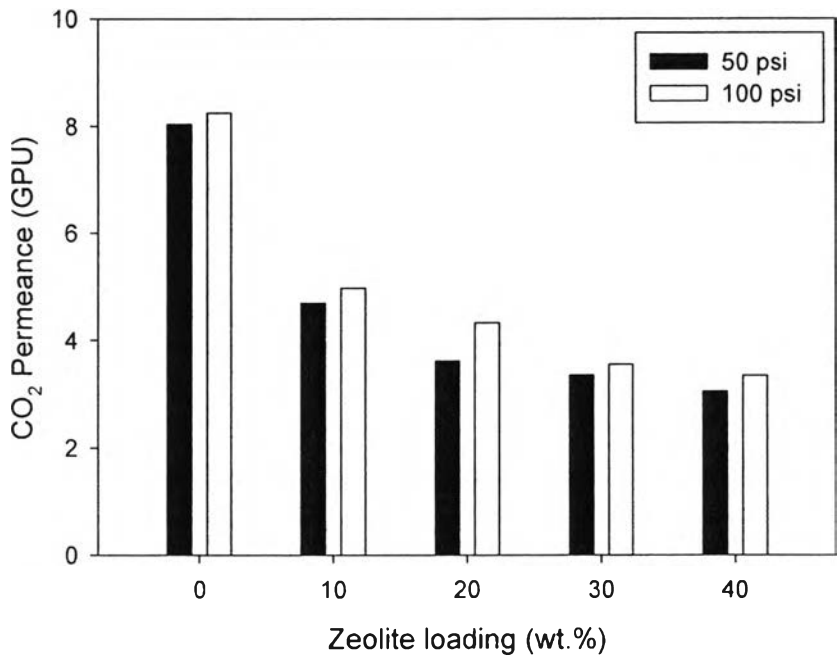

Figure 4.9 Effect of mordenite loading on CO_2 permeance at 50 and 100 psi feed.

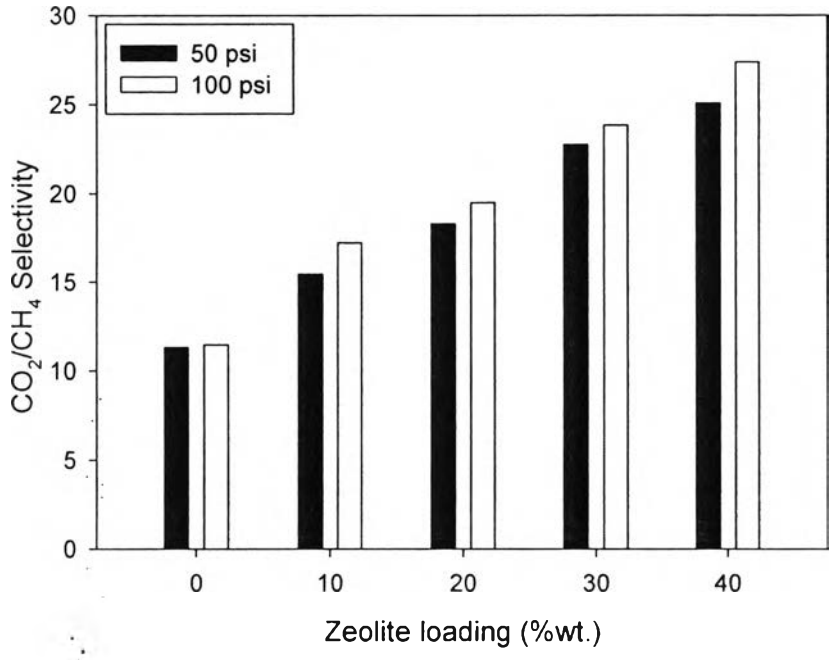

Figure 4.10 Effect of mordenite loading on CO_2/CH_4 selectivity at 50 and 100 psi feed.

Since pore opening of mordenite zeolite (3.9 Å) (Ackley *et al.*, 2003) is large than the kinetic diameters of CO_2 molecules (3.3 Å) and CH_4 molecules (3.8 Å), mordenite zeolite would not be able to discriminate CO_2 and CH_4 molecules based on size and shape. However, at a given feed pressure, the CO_2 permeance of MOR-CA MMMs was decreased with an increase in mordenite loading whereas their CO_2/CH_4 separation performance was increased with increasing mordenite content. This suggests that partial pore blockage of zeolites by polymer chains and polymer chain rigidification play important roles in separation performance of MOR-CA MMMs. These phenomena were also occurred with NaA-CA and CaA-CA MMMs.

The decrease in CO_2 and CH_4 permeances of MOR-CA MMMs can be explained that the CA polymer chain rigidification was induced by the presence of nearby mordenite zeolite (Li *et al.*, 2005). However, it should be noted that their CO_2 permeance is still higher than that of CH_4. This is because the combination of molecular sieving effect of partial blocked mordenite zeolite and condensable nature of CO_2 molecules facilitate CO_2 molecules to pass through MMMs easily when compared to that of CH_4 molecules.

From theses reasons, the CO_2/CH_4 selectivity was increased with increasing mordenite loading.

As shown in Figure 4.9, at the same zeolite loading, an increase in feed enhanced CO_2 permeance. Moreover, the CO_2/CH_4 selectivity also increased with the feed pressure, as shown in Figure 4.10. This signifies that although the diffusion driving force was raised for both tested gas molecules at a given zeolite loading; however Mor-CA MMMs still assist CO_2 molecules through membranes more than CH_4 molecules.

4.7 Modified Maxwell model

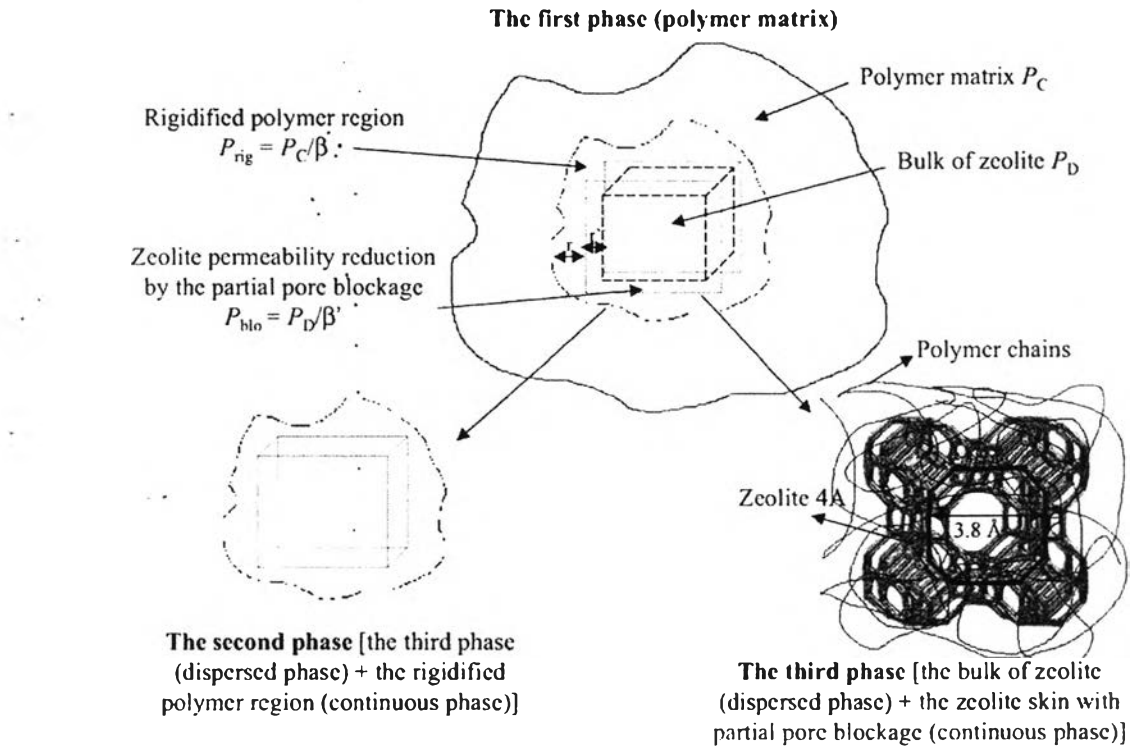

Figure 4.11 Schematic diagram of modified Maxwell model (Li *et al.*, 2005).

Li *et al.* (2005) proposed the modified Maxwell model to predict the gas transport property and separation performance of MMMs. The modified Maxwell model takes the combined effects of the polymer chain rigidification and partial pore blockage of zeolites into consideration. This model requires the intrinsic gas permeation properties of

zeolites to predict the gas separation performance of MMMs in the calculations. The modified Maxwell model is schematically shown in Figure 4.11

In their work, a decrease of O_2 and N_2 permeabilities and an increase in O_2/N_2 separation performance of NaA-PES MMMS with increasing NaA loading were attributed to the inhibition of polymer chain mobility near the polymer-zeolite interface and the partial pore blockage of zeolite by the polymer chains. In addition, the assessment of a new modified Maxwell model that combines the polymer chain rigidification and partial pore blockage into account demonstrated that the gas permeability and selectivity predicted form such a model showed a good agreement with the experimental data.

As previously discussed, since a decrease in CO_2 permeance and an increase in CO_2/CH_4 selectivity of NaA-CA, CaA-CA, and Mor-CA MMMs with increasing zeolite loading in this experiment may be due to the inhibition of polymer chain mobility near the polymer-zeolite interface and the partial pore blockage of zeolite by polymer chains; therefore, it is imperative to adopt that such phenomena would occur in NaA-CA, CaA-CA, and Mor-CA MMMs by comparing the CO_2 permeability and CO_2/CH_4 separation performance of these systems with those predicted from the modified Maxwell model. However, to date only O_2 and N_2 permeability data of zeolite NaA can be found in literature and relative consistency while there consistent CO_2 and CH_4 permeability data of zeolite NaA are seldom available. For the other zeolites studied, such as CaA, H-Mordenite, such data on gas permeability cannot be found in literature. With this reason, O_2 and N_2 permeabilities and O_2/N_2 selectivity for NaA-CA MMMs was carried out the effect of polymer chain rigidification and partial pore blockage for making comparisons with the values predicted by the modified Maxwell model.

In comparison of gas permeability obtained by the experiment and model, Figures 4.12 and 4.13 present the O_2 and N_2 permeabilities for NaA-CA MMMs, respectively. The results show that both N_2 and O_2 permeabilities generally decrease with an increase in NaA loading. Their magnitudes of permeability are significantly different. Since the pore size of NaA (3.8 Å) zeolite is larger than the kinetic diameters of O_2 (3.46 Å) and N_2 (3.64 Å), the decrease in permeability would be attributed to a decrease in mobility of polymer chains near the polymer-zeolite interface and the partial pore blockage of zeolite by the polymer chains.

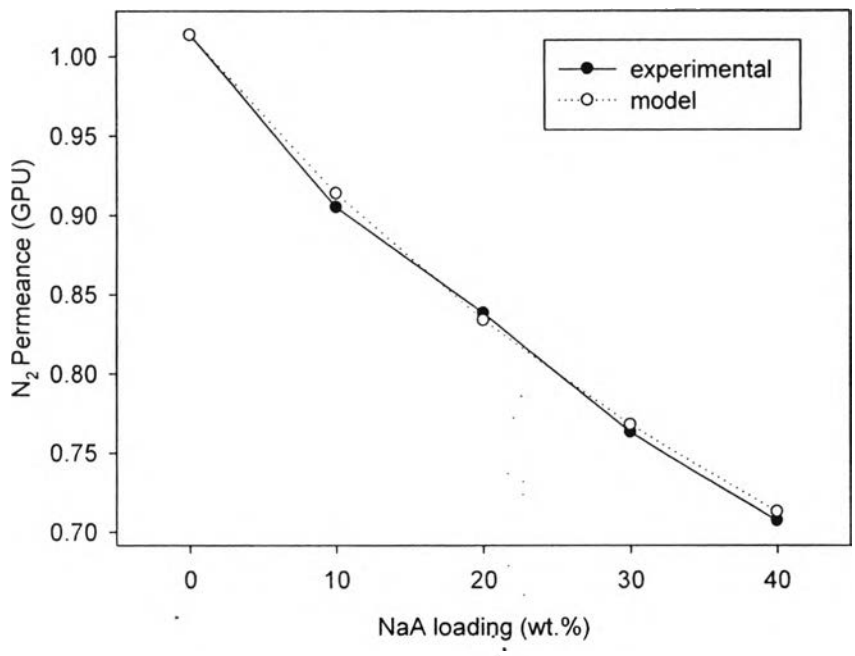

Figure 4.12 Comparison of N_2 permeability of NaA-CA MMMs based on experimental and modified Maxwell model data.

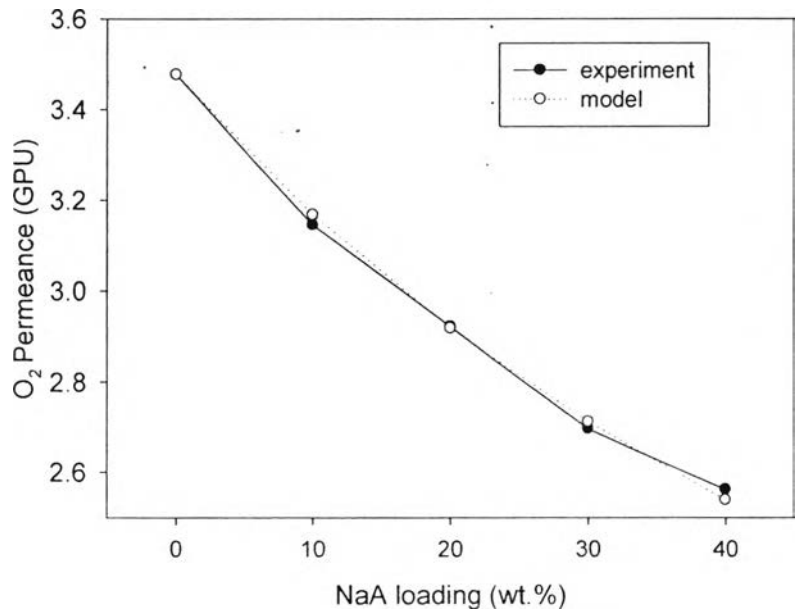

Figure 4.13 Comparison of O_2 permeances of NaA-CA MMMs based on experimental and modified Maxwell model data.

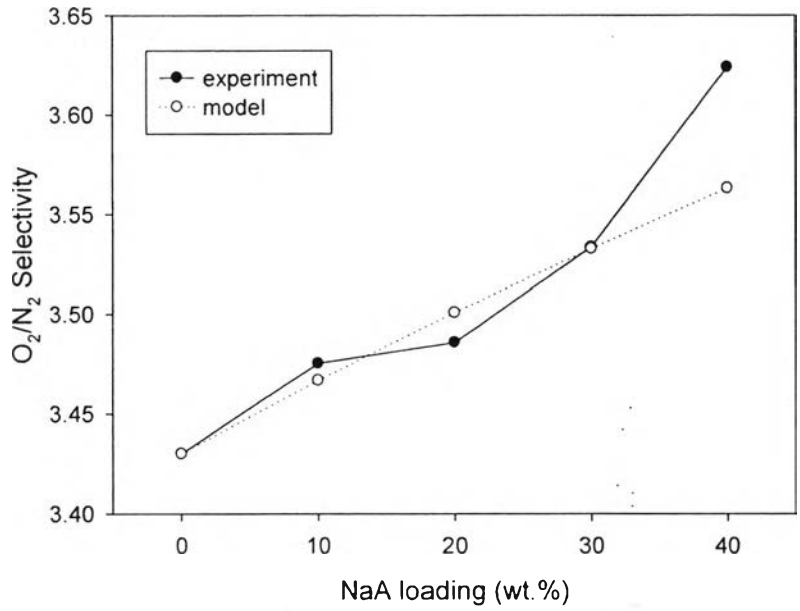

Figure 4.14 Comparison of O_2/N_2 selectivity of NaA-CA MMMs based on experimental and modified Maxwell model data.

As shown in Figure 4.14, the O_2/N_2 selectivity for NaA-CA MMMs is enhanced as NaA loading is increased. This is because the partial pore blockage of NaA zeolite by CA polymer chains occurs, resulting in decreasing pore opening below its nominal value; hence, NaA zeolite can exclude N_2 from O_2 more effectively (Mahajan, 1998 and Rallabandi *et al.*, 2000). Since the results are in good agreement with the values predicted by the modified Mxawell model, it is postulate that a decrease in CO_2 permeance and an increase in CO_2/CH_4 selectivity for NaA-CA, CaA-CA, and Mor-CA MMMs with increasing zeolite loading may be due to the inhibition of polymer chain mobility near the polymer-zeolite interface and the partial pore blockage of zeolite by polymer chains.